Nikola Pajerová; Ivana Linkeová
Triangular mesh analysis with application on hip bone

Persistent URL: http://dml.cz/dmlcz/703103

TRIANGULAR MESH ANALYSIS WITH APPLICATION ON HIP BONE

Nikola Pajerová, Ivana Linkeová

Department of Technical Mathematics, Faculty of Mechanical Engineering
Czech Technical University in Prague
Karlovo náměstí 13, 121 35 Praha 2
nikola.pajerova@fs.cvut.cz, Ivana.Linkeova@fs.cvut.cz

Abstract: Shape analyses and similarity measuring is a very often solved problem in computer graphics. The shape distribution approach based on shape functions is frequently used for this determination. The experience from a comparison of ball-bar standard triangular meshes was used to match hip bones triangular meshes. The aim is to find relation between similarity measures obtained by shape distributions approach.

Keywords: shape analyses, surfaces similarity, shape distribution, shape function

MSC: 65N15, 65M15, 65F08

1. Introduction

Application of shape distributions in shape analyses represents an efficient approach to compute similarity measures of 3D shapes. The digital shape characteristics are represented as a probability distribution sampled from a suitable shape function based on simple measurements of geometrical features, e.g. angles, distances, areas, volumes, mentioned in [3] and [4]. The probability distribution depicted in form of histogram polyline is called shape distribution is discussed [4] and [5]. This approach reduces the shape matching problem to the relatively simpler problem, i.e. comparison of two probability distributions instead of traditional shape matching methods, e.g. parametrization, feature correspondence and model fitting. The method for construction of shape distributions from 3D polygonal models to compute a measure of their dissimilarities consists of these steps: shape function selection, random points sampling, shape distributions calculation and shape distributions comparison. Shape distributions calculated for a sufficiently large number of random sample points of the surface are compared using Minkowski L_N norm.

In this paper, the shape distributions method is used to determine similarity between five triangular meshes of ball-bar standard in STL format obtained by optical

scanning and between few selected meshes of pubic symphysis of hip bones in STL format, too. The standard is made of two precise spheres connected by a cylinder (Fig. 1) and is used for calibration of optical scanners. The goal of this paper is to find the similarity measure between meshes obtained by the shape distributions approach and to verify the usability of these shape functions in pubic symphysis (part of hip bone, see Fig. 2) meshes similarity comparison.
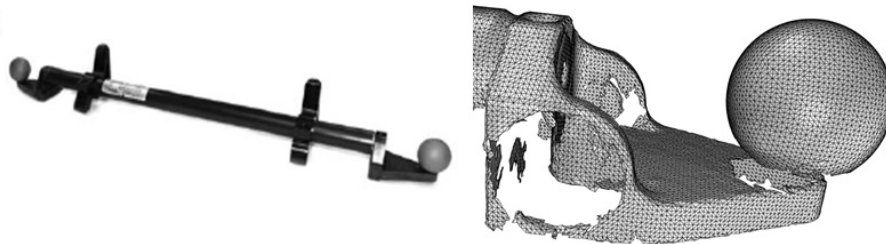

Figure 1: Ball-bar standard and a detail of the triangular mesh.

2. Meshes pre-processing and shape functions selection

The ball-bar meshes were oriented and inappropriate parts belonging to the handle of the sphere (Fig. 1) were removed as mentioned in [7].

In case of hip bones, the meshes were also aligned using Procrustes analysis (position and scale transformation for object alignment) to fit the scale and orientation above the plane xy ((Fig. 2)).
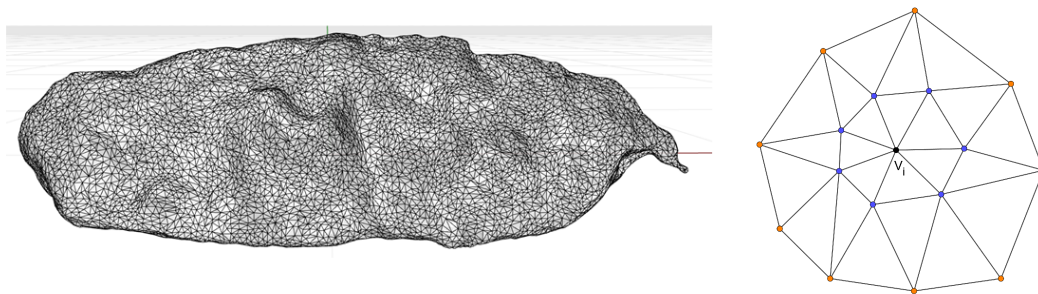

Figure 2: Pubic symphysis mesh of the 30 years old women pubic symphysis and 2-neighbourhood for mesh vertex V_i.

The shape function selection is the first step for construction of shape distributions. The modifications of $D1$, $D2$ and $D3$ shape functions described in [4] were used. The difference between modification and original shape function is as follows:

the original function works with points calculated randomly on a smooth surface, the modification works with input data (i.e. mesh vertices).

The modified shape function $D1$ measures the oriented distance of mesh vertex from origin, i.e.

$$f_i = \text{sign}(x_i)\sqrt{x_i^2 + y_i^2 + z_i^2}, \quad i = 0, 1, \ldots, n, \tag{1}$$

where for $\text{sign}(x_i) = 0$ the positive value is considered (the same in the following formulae).

The modification of $D2$ shape function measures the oriented distance between two mesh vertices, i.e.

$$\widehat{f_i} = \text{sign}(x_{S_i})\|\mathbf{a_i}\|, \quad i = 0, 1, \ldots, k, \tag{2}$$

where x_{S_i} is the x-coordinate of midpoint S for line segment V_iV_{i+1}, represented by vector a_i.

And modification of $D3$ shape function measures the oriented square root of triangle area with one vertex at origin and other vertices as mesh vertices, i.e.

$$\widetilde{f_i} = \text{sign}(x_{T_i})\sqrt{\frac{\|\mathbf{u_i} + \mathbf{v_i}\|}{2}}, \quad i = 0, 1, \ldots, l, \tag{3}$$

where x_{T_i} is the x-coordinate of triangle centroid and vectors u_i and v_i are directional vectors of two mesh vertices.

In order to use the shape function for hip bone, a new function $C2$ measuring the oriented curvature at a vertex of triangular mesh is introduced in this paper and is based upon the discrete Gaussian curvature from [1] or [2]. The oriented curvature at a vertex is done by the least square fitting of a sphere in 2-neighbourhood of the vertex (this neighbourhood is depicted in Fig. 2). This new shape function has a formula:

$$c_i = a(z)\frac{1}{r_{\text{sphere}}}, \quad i = 0, 1, \ldots, n, \tag{4}$$

where r_{sphere} is the radius of fitted sphere and $a(z)$ is a sign function, that returns -1 in case there are more points with lower z-coordinate than centre of sphere and $+1$ otherwise.

3. Shape distribution construction and its comparison

After shape function selection, a frequency histogram calculation was done, i.e., determination how many values f_i fall into each of k fixed sized classes. The frequencies were normalized by the number of mesh vertices n to eliminate the influence of different number of meshes vertices. This piecewise linear function constructed from the relative frequency histogram forms the representation for the shape distribution.

In case the shape distribution is represented by the relative frequency histogram, the similarity measurement is based on Minkowski L_1 norm

$$D(f, g) = \sum_{i=1}^{k} |f_i - g_i|, \qquad (5)$$

where f_i and g_i calculated according to (1) represent the relative frequency of two triangular meshes.

4. Experimental results

The shape distributions from $D1$-oriented shape function calculated for all triangular ball-bar meshes $M1$, $M2$,..., $M5$ are depicted in Fig. 3 (for better colour resolution of the individual series in the graphs, please see the online version). The resemblance of characteristics is obvious. The more the curves overlap the greater their similarity. And in correspondence: the grater the Minkowski L_1 norm value of two meshes the worse their similarity. The values of Minkowski L_1 norms for these shape distributions calculated according to (5) are displayed in Tab. 1: the minimal nonzero value $D_{\min} = 0.043506$ indicates the best similarity between $M3$ and $M4$. The maximal value $D_{\max} = 0.069793$ indicates the worst similarity of meshes $M2$ and $M4$ (both extrema are highlighted in bold in Tab. 1).

$D1$	M1	M2	M3	M4	M5
M1	0	0.055781	0.056787	0.066404	0.051121
M2	0.055781	0	0.059091	**0.069793**	0.053479
M3	0.056787	0.059091	0	**0.043506**	0.047324
M4	0.066404	0.069793	0.043506	0	0.053777
M5	0.051121	0.053479	0.047324	0.053777	0

Table 1: Comparison of D1-oriented shape distributions for ball-bar meshes.

$D2$	M1	M2	M3	M4	M5
M1	0	0.029904	0.030127	0.034288	0.020421
M2	0.029904	0	0.029683	**0.052911**	0.027332
M3	0.030127	0.029683	0	0.046253	**0.019839**
M4	0.034288	0.052911	0.046253	0	0.032937
M5	0.020421	0.027332	0.019839	0.032937	0

Table 2: Comparison of D2-oriented shape distributions for ball-bar meshes.

Resulted shape distributions from $D2$-oriented shape function of ball-bar triangular meshes $M1$, $M2$, ..., $M5$ are depicted in Fig. 3, too. The main values of
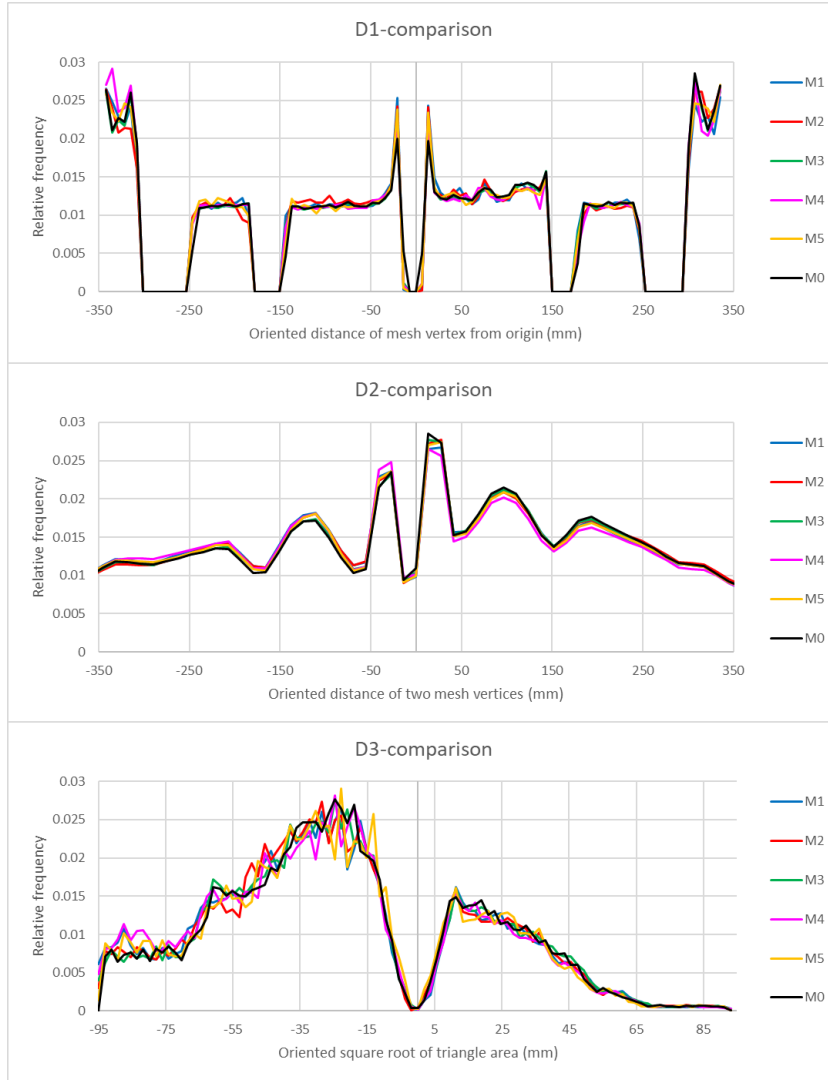
Figure 3: D1-, D2- and D3-oriented shape function for ball-bar.

Minkowski L_1 norms are: the minimal nonzero value $D_{\min} = 0.019839$ between $M3$ and $M5$ and the maximal value $D_{\max} = 0.052911$ between $M2$ and $M4$ (Tab. 2).

Similarly, the shape distributions from $D3$-oriented shape function calculated for ball-bar meshes are depicted in Fig. 3. The symmetry of the ball-bar is not as visible from these graphs as from the previous two. The important values of Minkowski L_1 norms are: minimal nonzero value is $D_{\min} = 0.068143$ between $M1$ and $M2$ and the maximal value is $D_{\max} = 0.11956$ between $M4$ and $M5$ (Tab. 3). The symmetry of the objects is visible from the symmetry of the shape distribution curve in all these graphs.
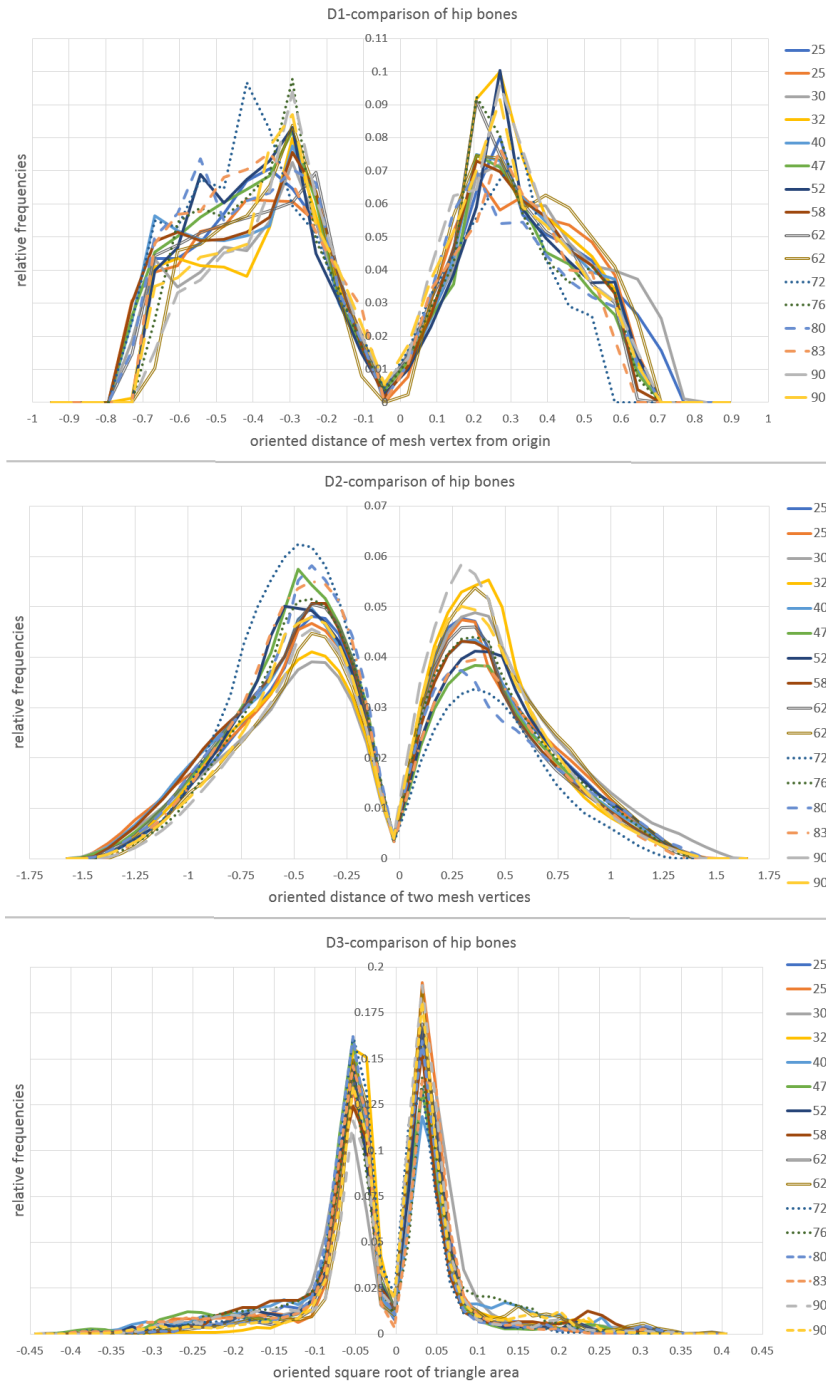
Figure 4: D1-, D2- and D3-oriented shape function for hip bones.

From minimal and maximal values of Minkowski L_1 norms and from the fact, that the meshes are obtained from the scanning of the same object, we can deduce,

$\boldsymbol{D3}$	M1	M2	M3	M4	M5
M1	0	**0.068143**	0.095878	0.090844	0.10116
M2	0.068143	0	0.096972	0.11021	0.11049
M3	0.095878	0.096972	0	0.096862	0.1188
M4	0.090844	0.11021	0.096862	0	**0.11956**
M5	0.10116	0.11049	0.1188	0.11956	0

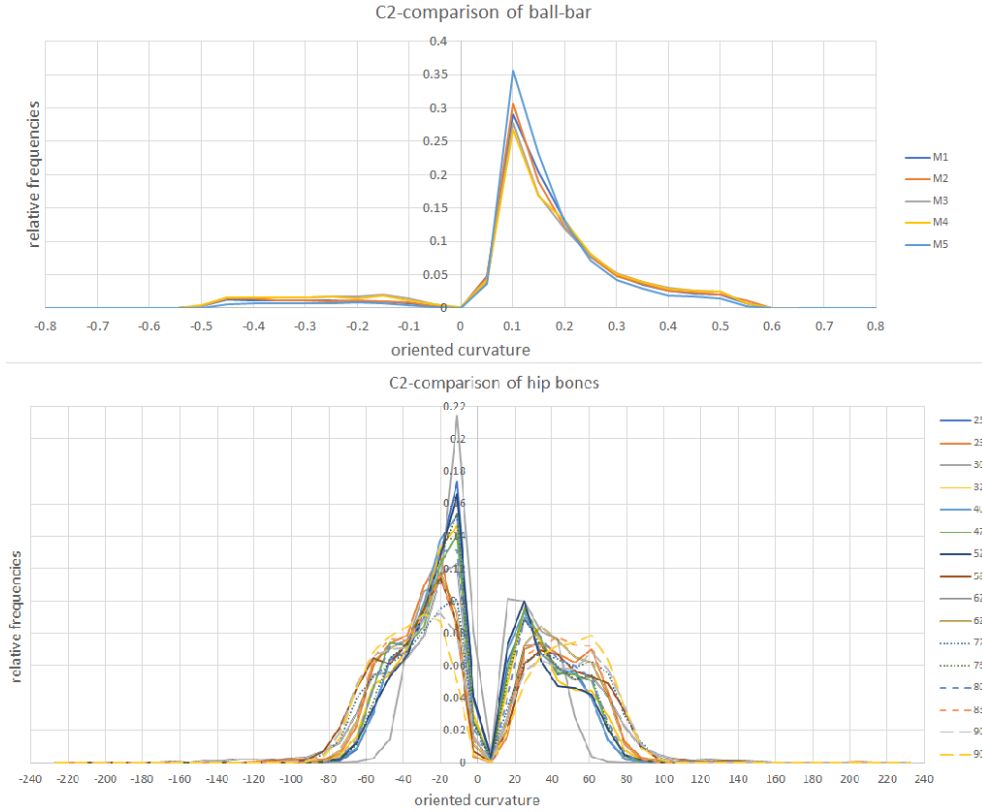Table 3: Comparison of D3-oriented shape distributions for ball-bar meshes.

Figure 5: C2-oriented shape function for ball-bar and hip bones.

that the $D3$ function is not so suitable for measuring the similarities as functions $D1$ and $D2$, because of great difference between $D_{\max}$ and $D_{\min}$ (for the first two shape functions the difference is about 0.03, but for the $D3$ it is almost 0.05). However, this fact can be caused by the noise in the data, so the exact result proving this deduction was made in [7] using MSA (Measurement System Analysis) method.

When using the $C2$-oriented shape function, the shape distributions of all ball-bar meshes are sketched in Fig. 5. The symmetry of the ball-bar is in this graph also very clearly visible. The values of Minkowski L_1 norms are: minimal nonzero value

$C2$	M1	M2	M3	M4	M5
M1	0	0.05552	0.14257	0.13542	0.18341
M2	0.05552	0	0.12706	0.13783	0.19473
M3	0.14257	0.12706	0	**0.046764**	0.29719
M4	0.13542	0.13783	0.046764	0	**0.30438**
M5	0.18341	0.19473	0.29719	0.30438	0

Table 4: Comparison of C2-oriented shape distributions for ball-bar meshes.

is $D_{\min} = 0.046764$ between $M3$ and $M4$ and the maximal value is $D_{\max} = 0.30438$ between $M4$ and $M5$ (Tab. 4).

The same procedure was applied to pubic symphysis meshes with results for $D1$ function depicted in Fig. 4, where the symmetry of the bones surfaces is obvious, but the course of these graphs are various. The $D2$ function demonstrates the symmetry of the bones, too. And for $D3$ function the symmetry and variance of bone surfaces is apparent. The last $C2$ function is depicted in Fig. 5 (tables for these functions are not included because of too many values). Its graphs show, that there is a tendency of graphs peaks to decrease with increasing age, that is more visible from the graph in Fig. 6. Additionally, the width of the peaks is getting wider when age increases.
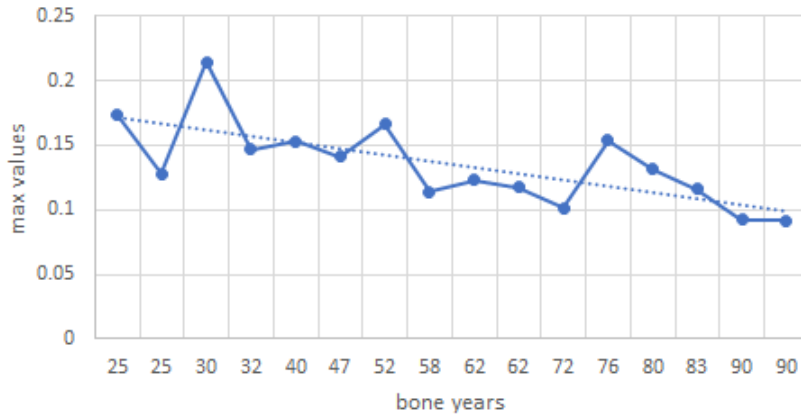

Figure 6: Graph of age dependence on the curvature values.

The important values of Minkowski L_1 norm for $D1$ function are: the lowest value is $D_{\min} = 0.05506$ between bones of ages 40 and 58 and the highest is $D_{\max} = 0.4272$ between bones 62 and 72.

The values of Minkowski L_1 norm for $D2$ function are: $D_{\min} = 0.11208$ between bones of ages 54 and 73 and $D_{\max} = 0.57928$ between bones 83 and 89.

The values of Minkowski L_1 norm for $D3$ function are: $D_{\min} = 0.085187$ between bones of ages 62 and 73 and $D_{\max} = 0.55654$ between bones 30 and 62.

And last values of Minkowski L_1 norm for $C2$ function are: the lowest value is $D_{\min} = 0.07287$ between bones of ages *62* and *83* and the highest is $D_{\max} = 0.87035$ between bones *30* and *90*. These norms correspond with the fact, that age has an impact on the structure of the pubic symphysis.

These values and shapes of graphs show, that function $C2$ is suitable for measuring the structure of bone roughness.

5. Conclusion

Shapes of ball-bar and bones characteristics of shape distributions show the difference between ball-bar shape and bone shape unambiguously for each shape function. It means, these functions are applicable to detect dissimilarity between different shapes. But the best functions for detecting the similarity of meshes from the same object are $D1$ and $D2$. For bone application, where the shapes are similar but the surfaces have a bit various structure, the best shape function is $C2$ is the best since it describes the roughness.

Acknowledgements

References

[1] Bobenko, A. I.: Geometry II – discrete differential geometry, April 21 (2020). Preliminary version for the summer semester 2020, page 12.

[2] Bobenko, A. I., Schröder, P., Sullivan, J. M., and Ziegler, G. M.: Discrete differential geometry, Vol. 38 (2000), page 180, Birkhäuser Verlag, Basel – Boston – Berlin.

[3] Monteverde, L. C., Ruiz, C. R., and Huang Z.: A shape distribution for comparing 3D models. In: *Advances in Multimedia Modeling*. MMM 2007. *Lecture Notes in Computer Science*, vol 4351. Springer, Berlin, Heidelberg.

[4] Osada, R., Fankhouser, T., Chazelle, B., and Dobkin, D.: Matching 3D models with shape distributions. In: Proceedings International Conference on Shape Modeling and Applications, Genova (2001).

[5] Osada, R., Fankhouser, T., Chazelle, B., and Dobkin, D.: Shape distributions. ACM Transactions on Graphics **21 (4)** (2002), 807–832.

[6] Pajerová, N. and Linkeová, I.: Application of shape distributions to compare triangular meshes. In: Proceedings APLIMAT 2018, 17th Conference on Applied Mathematics, (2018), 795–802.

[7] Pajerová, N., Linkeová, I.: Similarity of triangular meshes measurement. In: Proceedings APLIMAT 2019, 18th Conference on Applied Mathematics, (2018), 888–895.

[8] Yu, I. C., Lapadat, D., Sieger, L., and Regli, W. C.: Using shape distributions to compare solid models. In: Proceedings of the seventh ACM symposium on Solid modeling and applications (SMA '02). ACM, New York, NY, USA, 273–280.